Pelizaeus-Merzbacher like disease is caused not only by a loss of Connexin47 function but also by a hemichannel dysfunction

Simone Diekmann[1], Marco Henneke[1], Birgitta C. Burckhardt[2], and Jutta Gärtner*[,1]

[1]Department of Pediatrics and Pediatric Neurology, Georg August University, Göttingen, Germany

[2]Department of Physiology and Pathophysiology, Georg August University, Göttingen, Germany

*Correspondence:

Jutta Gärtner, M.D., Department of Pediatrics and Pediatric Neurology, Georg August University, Robert-Koch-Strasse 40, 37075 Göttingen, Germany, telephone number +49-551-398035, fax number +49-551-396252, e-mail gaertnj@med.uni-goettingen.de.

Running title: PMLD – Genetic and functional defects of Cx47

ABSTRACT

Autosomal recessive mutations in the *GJA12/GJC2* gene encoding the gap junction protein connexin47 (Cx47) cause a form of Pelizaeus-Merzbacher like disease (PMLD) with hypomyelination, nystagmus, impaired psychomotor development and progressive spasticity. We investigated the functional consequences of four Cx47 missense mutations (G149S, G236R, T265A, T398I) and one Cx47 complex mutation (A98G_V99insT) by immunoblot analysis and immunocytochemistry in transfected communication incompetent HeLa cells and in OLI-neu cells. All studied Cx47 mutants except G236R generated stable proteins in transfected HeLa cells and OLI-neu cells. T265A and A98G_V99insT were retained in the ER, T398I formed gap junctional plaques at the plasma membrane, and G149S showed both, structures at the plasma membrane and ER localization. Two-microelectrode voltage clamp analyses in *Xenopus laevis* oocytes injected with wild-type and mutant Cx47 cRNA revealed reduced hemichannel currents for G236R, T265A, and A98G_V99insT. In contrast, T398I revealed hemichannel currents comparable to wild-type. For Cx47 mutant T398I our results indicate a defect in hemichannel function, whereas Cx47 mutants G149S, G236R, T265A, and A98G_V99insT are predicted to result in a loss of Cx47 hemichannel function. Thus, PMLD is likely to be caused by two different disease mechanisms, a loss-of-function and a dysfunction.

Keywords: Leukodystrophy; Pelizaeus-Merzbacher like disease; GJA12/GJC2 mutations; connexin47; voltage clamp analysis

Introduction

Pelizaeus-Merzbacher Disease (PMD; MIM#312080), the prototype of hypo-myelinating disorders, is due to X-linked recessive rearrangements or mutations of the *proteolipid protein (PLP1)* gene.[1] Clinical features of the classical form comprise nystagmus and impaired psychomotor development within the first months of life followed by progressive spasticity and cerebellar signs. Pelizaeus-Merzbacher Like Disease (PMLD, MIM#608804) shows clinical and neuroradiologic features like classic PMD but is not associated with *PLP1* molecular defects.[2] Recessive mutations in the *GJA12* gene, recently renamed *GJC2* (http://www.genenames.org/genefamily/gj.php), cause one form of PMLD.[3] *GJA12/GJC2* encodes gap junction protein connexin47 (Cx47). Until now 23 different *GJA12/GJC2* mutations have been reported.[3-9]

Gap junctions (GJ) are specialized channels between apposed cells allowing direct metabolic and electrical communication between most cell types in mammalian tissues by passive diffusion of molecules smaller than 1000 Dalton. This gap junction intercellular communication (GJIC) plays an important role in essential cellular processes such as development, proliferation, differentiation, and cell death.[10] GJs are highly specialized structures, consisting of two hemi-channels of apposing cells. Up to several thousand GJ channels assemble to gap junctional plaques. The hemichannel (connexon) in the plasma membrane is formed by six connexins. Connexins, highly conserved integral membrane proteins, have four transmembrane domains, two extracellular loops and three cytoplasmic components, one amino- and carboxy-terminal region, and a cyto-plasmic loop. Homotypic GJs consist of hemichannels with one type of

connexins, whereas heterotypic GJs are formed by hemichannels with different connexins.[11] So far, 20 *connexin* genes have been described in mouse and 21 in human genome. More than half of them are expressed in the nervous system.[12]

Astrocytes and oligodendrocytes are coupled by GJs forming part of the "panglial syncytium".[13] GJIC occurs between oligodendrocytes and astrocytes (O/A) and adjacent astrocytes (A/A), but there is no evidence for GJs between adjacent oligodendrocytes in mice.[13-16] Oligodendrocytes express Cx47, Cx32, and Cx29,[16,17] whereas astrocytes express Cx26, Cx30, and Cx43.[18,19] O/A coupling is mediated by heterotypic channels between Cx47/Cx43 and Cx32/Cx30, both appearing to be essential for proper maintenance of myelin.[20] So far, Cx47 mutants have been shown to result in loss-of-function, suggesting an impaired O/A coupling mediated by Cx47/Cx43.[21] Here, we provide further evidence that loss of Cx47 function causes PMLD. However, our results further suggest a second disease mechanism, namely a Cx47 hemichannel dysfunction.

Materials and methods

Wild-type and mutant expression constructs. The full length Cx47 (1-1320 bp, 1-439aa, RefSeqID *NM_020435.2)* was PCR-amplified from wild-type cDNA and cloned into the mammalian expression vector pcDNA3.1+ (Invitrogen, Germany). Site-directed-mutagenesis was performed using the FlipFlop-Site-Directed-Mutagenesis-Kit (Bioline, Germany). Wild-type Cx47 with the alternative start-codon (10-1320bp, 4-439aa) was also cloned into pcDNA3.1+.

Generation of Cx47-antiserum. Polyclonal rabbit antiserum against human Cx47 was generated by conventional methods using GST-fusion protein as immunogen (Seramun, Germany). A fragment of the intracellular loop (310-591 bp, 104-197aa) was amplified using wild-type Cx47 construct as template. The PCR-product was subcloned into the pGEX-KG vector, which encodes for Glutathione-S-Transferase (GST). GST-fusion protein was expressed by BL21-bacteria (Bioline) and purified using glutathione-sepharose4B (GEHealthcare, Germany). Final bleed serum was used for immunoblot analysis at dilution 1:10000. This antiserum did not work properly in immunoblot analysis of oocyte lysates.

Immunoblot analysis. HeLa cells were cultured in Dulbecco's modified Eagle's medium containing 10% fetal bovine serum at 37°C and 5% CO_2. Transfection was done using the Effectene-Kit (Qiagen, Germany). Transfected HeLa cells were harvested 48 hours post-transfection and lysed in RIPA-buffer (in mM: 150 NaCl; 50 Tris-HCl; 5 EDTA; 0.5% Na-deoxycholate; 1% NP-40; 0.1% SDS; protease inhibitor cocktail). Immunoblot analyses were performed using standard techniques. Horseradish peroxidase conjugated secondary antibodies were used to visualize bound primary antibodies (Cx47-antiserum) with Lumi-Light Western-Blotting Substrate (Roche, Germany). Chemiluminescence signals were analyzed using the Luminescent-Image-Analyzer, LAS-4000mini (Fujifilm, Germany).

Immunocytochemistry. OLI-neu, an immortalized oligodendrocyte precursor cell line,[22] was cultured in Sato medium containing 1% horse serum on poly-(L-lysine) coated culture dishes at 37°C and 5% CO_2. OLI-neu cells were trans-

fected with FuGENE-HD (Roche, Germany). HeLa and OLI-neu cells transfected with wild-type or mutant Cx47 were fixed 20-48 hours post transfection with 4% paraformaldehyde/PBS. Immunostaining was done using standard methods with the Cx47-antiserum (dilution 1:2000) and with Pan-Cadherin (plasma membrane marker, Abcam, UK) and PDI (ER marker, Abcam) antibodies to detect colocalization. Alexa488- and Cy3-conjugated anti-rabbit and anti-mouse secondary antibodies were used (MolecularProbes, JacksonImmunoResearch, diluted 1:1000 and 1:500). The cells were embedded in ProLongGold mounting medium with DAPI (Invitrogen). Fluorescence signals were detected using fluorescence microscope Axio-Imager M.1 (Zeiss, Germany).

Oocyte preparation and microinjection. Stage V and VI oocytes from *Xenopus laevis* (Nasco, Fort Atkinson, WI) were seperated by treatment with collagenase (TypCLS II, Biochrom, Germany) and maintened at 16-18°C in daily replaced control solution (in mM): 110 NaCl, 3 KCl, 2 $CaCl_2$, 5 HEPES, pH 7.5, supplemented with sodium pyruvate (0,55 mg/ml) and gentamycin (50 µg/ml). An antisense oligonucleotide complementary to *Xenopus* Cx38 mRNA (asCx38) was synthesized: 5'-gctttagtaattcccatcctgccatgtttcc-3' (Metabion, Germany).[23] To deplete endogenous Cx38 expression asCx38 was injected (23 nl, 1 ng/nl) into oocytes one day after removal from the frog and 48-72 hours before recording. To analyze the function of Cx47 wild-type and mutant hemichannels in oocytes, cRNA transcription was performed in vitro, using the SP6 mMessage-mMachine-Kit (Ambion, USA). The cRNA (5 ng/oocyte) was coinjected with asCx38.

Electrophysiological studies. Resting membrane potentials and nonjunctional transmembrane currents in single oocytes were studied by two-electrode voltage clamp (TEVC) technique using a commercial amplifier (OC-725C, Warner, USA). The microelectrodes were filled with 3 M KCl and had resistances of less than 1MΩ. Oocytes were superfused with external bath solution (control solution without sodium pyruvate and gentamycin). After stabilization of the membrane potential, single oocytes were clamped to –40 mV. Superfusion was switched after 200 seconds to calcium-free bath solution. Nonjunctional transmembrane currents were measured after five minutes. A depolarisation pulse to 0 mV was applied to the oocyte and transmembrane currents were measured after 100 seconds. All currents were measured at a saturation of about 100% (see Supplementary Figure 1). At –40 mV calcium-activated chloride currents are mostly inactivated.[24] Channel opening is blocked by external divalent cations (i.e. Ca^{2+}) and in most cases by hyperpolarizing transmembrane potentials.[25]

The data were corrected by subtracting the average leakage current measured in control oocytes (only injected with asCx38). Some outliers were excluded using the Nalimov-outlier-test. An unpaired Student's t-test was probed.

Results

Expression of wild-type and mutant Cx47 in HeLa cells. We analyzed the functional consequences of four missense mutations G149S, G236R, T265A, and T398I as well as one complex mutation A98G_V99insT with an amino acid substitution followed by an amino acid insertion previously described.[7] The

localization within the different protein domains is illustrated in Figure 1 and is one criteria to study these five distinct missense mutations. To determine whether selected mutations affect protein expression, immunoblot analysis of transfected HeLa cells was performed (Figure 2). The wild-type and all mutants except G236R were detected by the Cx47-antiserum. There was no signal in untransfected HeLa cells, indicating the specificity of the Cx47-antiserum.

Intracellular localization of wild-type and mutant Cx47 in HeLa and OLI-neu cells. A second alternative Cx47 start-codon, nine nucleotides downstream from the first ATG, was described.[21] We analyzed expression and localization of the constructs with the first and the second start-codon by immunostaining of transfected HeLa and OLI-neu cells. Cx47 proteins were immunolabeled with the Cx47-antiserum and visualized using epifluorescence microscopy (Figure 3). There was no difference in subcellular localization both proteins were found in punctate structures localized to the plasma membrane. Therefore, all constructs analyzed in this study were cloned starting from the first ATG. Accordingly, our description of nucleotide and amino acid positions including the designation of mutations refers to the first upstream ATG.

To examine whether the Cx47 mutants were properly targeted to the plasma membrane, HeLa and OLI-neu cells transfected with one of the mutant constructs were immunolabeled with the Cx47-antiserum (Figure 4 and 5). Double staining immunofluorescence studies revealed differences in the subcellular localization of Cx47 mutants compared to wild-type protein. As expected, wild-type Cx47 was found in punctate structures colocalizing to the plasma membrane. These structures are assumed to represent gap junctional

plaques. T398I was labeled as punctate structures predominantly at the plasma membrane (Figure 4 A and 5 A). However, there was also faint colocalization to the ER. HeLa and OLI-neu cells expressing G149S showed punctate structures at the plasma membrane as well as in the ER (Figure 4 B and 5 B). A98G_V99insT and T265A were only localized to the ER (Figure 4 C, D and 5 C,D). As expected, there was no fluorescence signal in G236R transfected (Figure 4 E and 5 E) and in untransfected HeLa and OLI-neu cells (data not shown).

Functional characterization of wild-type and mutant Cx47 in *Xenopus laevis* oocytes. Resting membrane potentials and nonjunctional trans-membrane currents in single oocytes were studied by two-electrode voltage clamp (TEVC) technique. Average resting membrane potentials upon superfusion with calcium-containing solution for oocytes injected with asCx38 and wild-type Cx47 cRNA (WT) or mutant Cx47 cRNA (G149S, A98G_V99insT, G236R, and T265A) ranged from –35.4±0.8 mV to – 39.2±0.9 mV (Figure 6 A). There was no significant change of resting membrane potential compared to wild-type; only for those 84 oocytes injected with T398I a significant decreased potential was observed (–30.4±0.9 mV, P=0.0001). Resting membrane potential from 79 control oocytes showed a small significant hyperpolarisation (–41.9±0.9 mV, compared to wild-type –39.2±0.9 mV, P=0.025). The injected oocytes were clamped to –40 mV and superfused with calcium-free solution. They showed slowly activated inward currents that were reversibly inactivated when calcium-free solution was replaced. The amplitude of wild-type calcium-sensitive hemichannel currents after subtracting the average leakage current measured

in control oocytes was –554±49 nA (ΔI_m, Figure 6 B). In T398I injected oocytes ΔI_m represented –693±58 nA. There is no significant difference between corrected wild-type and T398I hemichannel currents (P=0.0826). Significantly reduced transmembrane currents were observed for G149S, A98G_V99insT, G236R, and T265A (P≤0.0012, compared to wild-type). Application of depolarization step to 0 mV elicited an instantaneous increment of outward calcium-sensitive currents in oocytes, injected with wild-type Cx47 cRNA (ΔI_m=406±36 nA, Figure 6 C). No depolarizing activation was observed for T398I hemichannel currents average (ΔI_m=162±18 nA). Transmembrane currents observed for G149S, A98G_V99insT, G236R, and T265A were significantly reduced (below 75 nA; P=0.0001). The transmembrane currents varied considerably in magnitude indicating that conductance of oocytes changed according to the cRNA injected.

Discussion

A second alternative start-codon for Cx47, nine nucleotides downstream from the first ATG, was described.[21] So far, there is no experimental evidence, which ATG of Cx47 is the translation initiation codon. Therefore, we analyzed expression and subcellular localization of both using constructs with the first and the second start-codon. Interestingly, we saw no difference in subcellular localization. Both proteins localized to the plasma membrane in HeLa cells. Whether one or both start-codons are translated and whether the downstream ATG is more favourable is still unknown.[26] Furthermore, it needs to be investigated whether a tissue specific translation exists. Reference sequence

NM_020435.2 (*NCBI database*) declares the upstream ATG to be the putative start-codon. All constructs analyzed in this study were cloned starting from the first ATG.

Besides G149S, all studied missense mutations affect highly conserved amino acids indicating evolutionary constrained key residues for protein function.[7] All Cx47 mutants except G236R were able to generate stable proteins in transfected HeLa cells. G236R leads to an amino acid substitution of neutral glycine against alkaline arginine in the second highly conserved extracellular domain. There are six highly conserved cysteines in both extracellular domains thought to be essential for connexin stabilization, connexin formation, and connexon docking.[27] The G236R substitution is closely located to C245. Presumably, this mutation inhibits formation of an important disulfide bond and leads to instability of Cx47 resulting in early degradation during translation. The degradation results in lack of this protein in the plasma membrane and may inhibit Cx47/Cx43 heterotypic GJIC between oligodendrocytes and astrocytes.[20] For PMD it was shown that mutations mapping into the extracellular loop region of PLP/DM20 lead to the failure of oligodendrocytes to form correct intramolecular disulfide bonds and result in activation of the unfolded protein response (UPR).[28] Interestingly, point mutations in the second extracellular domain of Cx43 are known to cause Oculodentodigital Dysplasia (ODDD) preventing Cx43 localization to the plasma membrane and consecutive loss-of-function.[29]

T398I, located in the C-terminus, does not alter the localization of Cx47 to the plasma membrane and apparently does not inhibit hemichannel function. The C-terminus contains multiple phosphorylatable serine, threonine, and tyrosine

residues that are considered an intrinsic part of the voltage and low pH gate for various GJ channels.[30] C-terminal mutations in the *Cx43* gene were identified in patients with heart malformation and defects in laterality.[31] In these cases one or more C-terminal phosphorylatable serine or threonine residues were substituted. Mutant transfectants were demonstrated to have normal levels of GJIC but abnormalities in its regulation. Furthermore, mutations in the C-terminus of *Cx32* are thought to affect functional regulation of GJs.[32,33] Using TEVC we saw depolarization of resting membrane potential in oocytes injected with T398I. This observation leads to the hypothesis that T398I hemichannel opening occurs incidentally. Consequently this mutant may affect oligodendrocytes causing leakage across the plasma membrane through opening hemichannels. Presence of open hemichannels was shown for other connexins and postulated as a possible mechanism of cell-injury and -death in other tissues.[34,35] Therefore, a regulation defect of Cx47 hemichannel function in mutant T398I is likely.

Mutation G149S lies within the less conserved intracellular protein domain. It colocalized to the ER and partially also to the plasma membrane. Hemichannel currents were nearly absent. The weak transmembrane currents could be caused by formation of nonfunctional hemichannels, by aggregation of connexins in the ER preventing the assembling of hemichannels at the plasma membrane, or by unspecific currents higher than those for control oocytes. Faint transmembrane currents were also observed for other mutants localized to the ER (T265A and A98G_V99insT) as well as for G236R, which did not express any protein product. Thus, these currents represent rather unspecific currents.

T265A and A98G_V99insT, both located in the transmembrane domains, showed significantly reduced hemichannel currents and were not able to form homomeric hemichannels. Both were retained in the ER. P90S, Y272D, and M286T, also located close to or directly at the transmembrane domains, showed aggregation of mutated connexins in the ER and loss of Cx47 function.[21] For the transmembrane domains three and four of Cx32 an important role in protein trafficking has been proposed.[36] Therefore mutations in the transmembrane domains of Cx47 might basically inhibit protein transport.

Two alternative pathomechanisms are considered to be responsible for GJA12/GJC2-associated PMLD. Like several previously described alterations our mutants G149S, G236R, T265A, and A98G_V99insT cause PMLD most likely by loss of Cx47 function. In contrast, T398I does not lead to loss-of-function but might result in a hemichannel dysfunction indicating a second and novel disease mechanism in GJA12/GJC2-associated PMLD.

Clinical features of patients carrying the characterized mutations previously described by our group are listed in table 1. Mutations G149S, T265A and A98G_V99insT were found at heterozygous state in four families; thus a genotype-phenotype correlation cannot be done for these alterations as the second allele may modulate the expression of the first one. Mutations T265A and G236R were identified at homozygous state in two families. Both alterations result indeed in a loss of Cx47 function, but only mutant G236R was not detected as stable protein in our experiments. The residual protein expressed for mutant T265A likely results in the milder phenotype of subject G330. However, more homozygous patients and the functional consequences of their

mutations must be analyzed in order to definitely assess a genotype-phenotype correlation in this disorder.

Mutants P90S, Y272D, and M286T do not efficiently form functional heterotypic Cx47/Cx43 GJs suggesting that disruption of these channels affects human myelination and cause GJA12/GJC2-associated PMLD.[20,37] Mice lacking Cx47 were viable and fertile and showed no obvious morphological or behavioral abnormalities,[17] whereas animals lacking Cx47 and Cx32 developed a profound CNS demyelination.[16] Potentially Cx30/Cx32 could compensate the lack of Cx43/Cx47 GJs in mice.[20] However, there is no evidence for such a compensatory mechanism in humans. Furthermore, Cx47/Cx43 and Cx32/Cx30 channels were described to have different roles in O/A coupling in primates.[37] Thus, PMLD is likely caused by loss-of-function for mutants expressing no proteins as well as for mutants retained in the ER. However, mutants assembling in the ER, as shown for T265A and A98G_V99insT in our study and as previously shown for P90S, Y272D, and M286T,[21] could also induce a pathological activation of UPR resulting in changes of cell physiology (i.e. apoptosis, abnormal differentiation, and altered proliferation). Although no experimental evidence for this putative pathomechanism was found in a cell model system analyzing the PERK-UPR pathway, the authors did not rule out that Cx47 activates a different UPR-related pathway.[21] For PLP1 mutants causing PMD and for mutants of peripheral myelin protein (PMP22) causing Charcot-Marie-Tooth type 1A (CMT1A) chronic, pathological activation of UPR by accumulation of misfolded and undegraded proteins in the ER has been postulated. [38-41] The activation of UPR by certain PLP1 mutants may result in

oligodendrocyte cell death affecting the myelination process.[42] Toxic accumulation of Cx32 in the ER has also been suggested as a pathomechanism for some X-linked Charcot-Marie-Tooth (CMTX) Cx32 mutants.[36] These authors postulated that inherited diseases of myelin share common pathophysiology in which mutant protein retained in intracellular compartments has deleterious effects on the protein folding, degradation, or trafficking machineries. Potentially there is coaction of both, loss of ability to form O/A heterotypic GJs and toxic ER accumulation. Moreover it is possible that oligodendrocyte and astrocyte connexins have roles besides forming GJs.[37] The O/O coupling in humans has not been examined, so it might be possible that Cx47 GJs exist between adjacent oligodendrocytes unlike shown in rodents.[37] In addition to Cx47/Cx43 dysfunction, abnormal homotypic Cx47 GJs between oligodendrocytes and myelin sheets could be responsible for the hypomyelination observed in PMLD patients.

Recently, complicated hereditary spastic paraplegia has been described as a novel milder phenotype for Cx47 mutation I33M.[8] The mutant formed homotypic gap junctional plaques in HeLa cells but formed altered heterotypic channels with Cx43 in a cell model system. The authors predict that I33M causes loss-of-function and disrupts GJIC via Cx47/Cx43 channels. If I33M has the same functional consequences as other mutations, another mechanism must account for the milder phenotype described.[8]

Finally, we could demonstrate a novel alternative PMLD pathomechanism, namely a Cx47 hemichannel dysfunction caused by a mutation localized in the C-terminus. Further studies of C-terminal mutations will contribute to a better

understanding of pathomechanisms in PMLD.

Acknowledgements

We thank Jens Kaiser and Irmgard Markmann for technical assistance and Hauke Werner and Patricia De Monasterio for providing OLI-neu cells. This study was supported by the Deutsche Forschungsgemeinschaft grant number GA354/6-1 (to J.G. and M.H.).

Conflict of interest

None.

Supplementary information is available at European Journal of Human Genetics website (http://www.nature.com/ejhg).

References

1. Saugier-Veber P, Munnich A, Bonneau D, et al. X-linked spastic paraplegia and Pelizaeus-Merzbacher disease are allelic disorders at the proteolipid protein locus. Nat Genet 1994; **6**: 257-262.

2. Schiffmann R, Boespflug-Tanguy O. An update on the leukodystrophies. Curr Opin Neurol 2001; **14**: 789-794.

3. Uhlenberg B, Schuelke M, Rüschendorf F, et al. Mutations in the gene encoding gap junction protein alpha 12 (connexin 46.6) cause Pelizaeus-Merzbacher-like disease. Am J Hum Genet 2004; **75**: 251-260.

4. Bugiani M, Al Shahwan S, Lamantea E, et al. GJA12 mutations in children with recessive hypomyelinating leukoencephalopathy. Neurology 2006;

67: 273-279.

5. Salviati L, Trevisson E, Baldoin MC. A novel deletion in the GJA12 gene causes Pelizaeus-Merzbacher-like disease. Neurogenetics 2007; **8**: 57-60.

6. Wolf NI, Cundall M, Rutland P, et al. Frameshift mutation in GJA12 leading to nystagmus, spastic ataxia and CNS dys-/demyelination. Neurogenetics 2007; **8**: 39-44.

7. Henneke M, Combes P, Diekmann S, et al. GJA12 mutations are a rare cause of Pelizaeus-Merzbacher-like disease. Neurology 2008; **70**: 748-754.

8. Orthmann-Murphy JL, Salsano E, Abrams CK, et al. Hereditary spastic paraplegia is a novel phenotype for GJA12/GJC2 mutations. Brain 2009; **132**: 426-438.

9. Wang J, Wang H, Wang Y, Chen T, Wu X, Jiang Y. Two novel gap junction protein alpha 12 gene mutations in two Chinese patients with Pelizaeus-Merzbacher-like disease. Brain Dev 2009; **32**: 236-243.

10. Trosko JE, Ruch RJ. Cell-cell communication in carcinogenesis. Front Biosci 1998; **3**: D208-D236.

11. Kumar NM, Gilula NB. The gap junction communication channel. Cell 1996; **84**: 381-388.

12. Nagy JI, Dudek FE, Rash JE. Update on connexins and gap junctions in neurons and glia in the mammalian nervous system. Brain Res Brain Res Rev 2004; **47**: 191-215.

13. Rash JE, Yasumura T, Dudek FE, Nagy JI. Cell-specific expression of connexins and evidence of restricted gap junctional coupling between glial cells and between neurons. J Neurosci 2001; **21**: 1983-2000.

14. Massa PT, Mugnaini E. Cell junctions and intramembrane particles of astrocytes and oligodendrocytes: a freeze-fracture study. Neuroscience 1982; **7**: 523-538.

15. Nagy JI, Ochalski PAY, Li J, Hertzberg EL. Evidence for the colocalization of another connexin with connexin-43 at astrocytic gap junctionsin rat brain. Neuroscience 1997; **78**: 533-548.

16. Menichella DM, Goodenough DA, Sirkowski E, Scherer SS, Paul DL. Connexins are critical for normal myelination in the CNS. J Neurosci 2003; **23**: 5963-5973.

17. Odermatt B, Wellershaus K, Wallraff A, et al. Connexin 47 (Cx47)-deficient mice with enhanced green fluorescent protein reporter gene reveal predominant oligodendrocytic expression of cx47 and display vacuolized myelin in the cns. J Neurosci 2003; **23**: 4549-4559.

18. Giaume C, Fromaget C, El Aoumari A, Cordier J, Glowinski J, Gros D. Gap junctions in cultured astrocytes: single-channel currents and characterization of channel-forming protein. Neuron 1991; **6**: 133-143.

19. Nagy JI, Li X, Rempel J, et al. Connexin26 in adult rodent central nervous system: demonstration at astrocytic gap junctions and colocalization with connexin30 and connexin43. J Comp Neurol 2001; **441**: 302-323.

20. Orthmann-Murphy JL, Freidin M, Fischer E, Scherer SS, Abrams CK. Two distinct heterotypic channels mediate gap junction coupling between astrocyte and oligodendrocyte connexins. J Neurosci 2007 b; **27**: 13949-13957.

21. Orthmann-Murphy JL, Enriquez AD, Abrams CK, Scherer SS. Loss-of-function GJA12/Connexin47 mutations cause Pelizaeus-Merzbacher-like

disease. Mol Cell Neurosci 2007 a; **34**: 629-641.

22. Jung M, Krämer E, Grzenkowski M, et al. Lines of murine oligodendroglial precursor cells immortalized by an activated neu tyrosine kinase show distinct degrees of interaction with axons in vitro and in vivo. Eur J Neurosci 1995; **7**: 1245-1265.

23. Barrio LC, Suchyna T, Bargiello T, et al. Gap junctions formed by connexins 26 and 32 alone and in combination are differently affected by applied voltage. Proc Natl Acad Sci U S A 1991; **88**: 8410-8414.

24. Barish ME. A transient calcium-dependent chloride current in the immature Xenopus oocyte. J Physiol 1983; **342**: 309-325.

25. Ebihara L. New roles for connexons. News Physiol Sci 2003; **18**:100-103.

26. Kozak M. Interpreting cDNA sequences: some insights from studies. Mamm Genome 1996; **7**: 563-574.

27. Foote CI, Zhou L, Zhu X, Nicholson BJ. The pattern of disulfide linkages in the extracellular loop regions of connexin 32 suggests a model for the docking interface of gap junctions. J Cell Biol 1998; **140**: 1187-1197.

28. Dhaunchak AS, Nave KA. A common mechanism of PLP/DM20 misfolding causes cysteine-mediated endoplasmic reticulum retention in oligodendrocytes and Pelizaeus-Merzbacher disease. Proc Natl Acad Sci USA 2007; **104**: 17813-17818.

29. Olbina G, Eckhart W. Mutations in the second extracellular region of connexin 43 prevent localization to the plasma membrane, but do not affect its ability to suppress cell growth. Mol Cancer Res 2003; **1**: 690-700.

30. Moreno AP, Lau AF. Gap junction channel gating modulated through

protein phosphorylation. Prog Biophys Mol Biol 2007; **94**: 107-119.

31. Britz-Cunningham SH, Shah MM, Zuppan CW, Fletcher WH. Mutations of the connexin 43 gap-junction gene in patients with heart malformations and defects of laterality. New Engl J Med 1995; **332**: 1323-1329.

32. Omori Y, Mesnil M, Yamasaki H. Connexin 32 Mutations from X-linked Charcot-Marie-Tooth Disease Patients: Functional Defects and Dominant Negative Effects. Mol Biol Cell 1996; **7**: 907-916.

33. Castro C, Gómez-Hernandez JM, Silander K, Barrio LC. Altered formation of hemichannels and gap junction channels caused by c-terminal connexin32 mutations. J Neurosci 1999; **19**: 3752-3760.

34. Kondo RP, Wang SY, John SA, Weiss JN, Goldhaber JI. Metabolic inhibition activates a non-selective current through connexin hemichannels in isolated ventricular myocytes. J Mol Cell Cardiol 2000; **32**: 1859-1872.

35. Liang GS, de Miguel M, Gómez-Hernández JM, et al. Severe Neuropathy with Leaky Connexin32 Hemichannels. Ann Neurol 2005; **57**: 749-754.

36. Deschênes SM, Walcott JL, Wexler TL, Scherer SS, Fischbeck KH. Altered trafficking of mutant connexin32. J Neurosci 1997; **17**: 9077-9084.

37. Orthmann-Murphy JL, Abrams CK, Scherer SS. Gap junctions couple astrocytes and oligodendrocytes. J Mol Neurosci 2008; **35**: 101-116.

38. Gow A, Lazzarini RA. A cellular mechanism governing the severity of Pelizaeus-Merzbacher disease. Nat Genet 1996; **13**: 422-428.

39. Gow A, Southwood CM, Lazzarini RA. Disrupted proteolipid protein trafficking results in oligodendrocyte apoptosis in an animal model of Pelizaeus-Merzbacher disease. J Cell Biol 1998; **140**: 925-934.

40. D'Urso D, Prior R, Greiner-Petter R, Gabreëls-Festen AA, Müller HW. Overloaded endoplasmic reticulum-Golgi compartments, a possible patho-mechanism of peripheral neuropathies caused by mutations of the peripheral myelin protein PMP22. J Neurosci 1998; **18**: 731-740.

41. Aridor M, Balch WE. Integration of endoplasmic reticulum signaling in health and disease. Nat Med 1999; **5**: 745-751.

42. Gow A, Friedrich VL, Lazzarini RA. Many naturally occurring mutations of myelin proteolipid protein impair its intracellular transport. J Neurosci Res 1994; **37**: 574-583.

Titles and legends to figures

Figure 1 Membrane topology and localization of all known *GJA12/GJC2* mutations. Seven mutations are observed on the four membrane-spanning domains, six on the intracellular loop, four on the extracellular loop, and six on the cytoplasmic carboxy-terminus. The five mutations characterized in this study are encircled. Mutations are designated according to current guidelines of international mutation nomenclature. Designation of the mutation p.P305RfsX155[6] and of the mutation p.P73AfsX35[9] was changed according to current guidelines of mutation nomenclature.

Figure 2 Immunoblot analysis of Cx47 expression in transfected communication incompetent HeLa cells. Immunoblot analysis was probed with HeLa cells transiently transfected with wild-type Cx47 (Cx47WT), mutant Cx47 (T398I, G149S, A98G_V99insT, G236R and T265A) and with untransfected HeLa cells (HeLa). Immunoblots were probed with a rabbit antiserum against human Cx47 (1:10000) and a monoclonal GAPDH antibody (Abcam, 1:5000).

Figure 3 Subcellular localization of wild-type Cx47. Double-staining immunofluorescence microscopy studies in communication incompetent HeLa cells (A,B) and OLI-neu cells (C,D) transiently transfected with wild-type Cx47 first ATG (Cx47WT, A, C) and alternative second ATG (Cx47WT2.ATG, B, D). Transfected cells were immunolabeled with a rabbit antiserum against human Cx47 (green) and a mouse monoclonal antibody against the plasma membrane

protein Pan-Cadherin (red). Gap junctional plaques were seen at the plasma membrane for cells expressing wild-type Cx47 from the first ATG as well as for cells expressing wild-type Cx47 from the alternative second ATG.

Figure 4 Subcellular localization of mutant Cx47 in HeLa cells. Communication incompetent HeLa cells transiently transfected with mutant Cx47 (T398I, G149S, A98G_V99insT, T265A and G236R) were immunolabeled with a rabbit antiserum against human Cx47 (green) and a mouse monoclonal antibody against the ER protein disulfide isomerase (α PDI, red). Gap junctional plaques were seen at the plasma membrane for cells expressing mutant T398I and G149S (A and B). There was also partial colocalization with the ER marker for both mutants, but the ER colocalization was even higher for the mutant G149S. Nearly perfect ER colocalization was seen for the mutants A98G_V99insT and T265A (C and D). As expected, there was no signal for mutant G236R (E).

Figure 5 Subcellular localization of mutant Cx47 in OLI-neu cells. OLI-neu cells transiently transfected with mutant Cx47 (T398I, G149S, A98G_V99insT, T265A and G236R) were immunolabeled with a rabbit antiserum against human Cx47 (green) and a mouse monoclonal antibody against the ER protein disulfide isomerase (α PDI, red). Like in HeLa cells gap junctional plaques were observed at the plasma membrane for OLI-neu cells expressing mutant T398I and G149S (A and B). There was also partial colocalization with the ER marker for both mutants, but the ER colocalization was even higher in the mutant G149S. Nearly perfect ER colocalization was seen for the mutants

A98G_V99insT and T265A (C and D). As expected, no signal for mutant G236R could be detected (E).

Figure 6 Electrophysiological studies of oocytes injected with wild-type and mutant Cx47 cRNA. Resting membrane potentials and nonjunctional transmembrane currents were measured by two-electrode voltage-clamp techniques. Resting membrane potentials (V_m) were recorded in control oocytes (co, injected with asCx38 only, n=79), wild-type (WT, n=84) and mutant (T398I, n=84; G149S, n=37; A98G_V99insT, n=34; G236R, n=40; and T265A, n=53) Cx47 expressing oocytes (additionally injected with asCx38) during perfusion with calcium containing solution (**A**). Membrane currents were monitored in control oocytes, wild-type and mutant Cx47 expressing oocytes (additionally injected with asCx38) clamped at –40 mV (**B**) or at 0 mV (**C**) during perfusion with calcium-free solution. All experimental data are averages of different numbers of oocytes (n=34-84) from at least three different donors. The data were corrected for leakage by subtracting the average leakage current measured in control oocytes (ΔI_m). Statistical analysis was done by an unpaired Student's t-test compared to wild-type. Errors are given as standard error of the mean (S.E.M.). The p-values (*P≤0.026; **P≤0.0032; ***P=0.0001) were adjusted according to Bonferroni.

Frameshift mutations

1 p.L28RfsX16[7]
4 p.P131RfsX79[7]
5 p.H132PfsX13[4]
7 p.E207GfsX3[7]
14 p.L281AfsX5[4]
16 p.P305RfsX155[5,6]
17 p.C318PfsX160[7]
18 p.A325PfsX147[7]
19 p.P330RfsX141[3]
21 p.R125SfsX12
25 p.P73AfsX35[9]

Missense mutations

2 p.P90S[3]
6 p.G149S[7]
9 p.G236R[7]
10 p.G236S[4]
12 p.T265A[7]
13 p.Y272D[3]
15 p.M286T[3]
20 p.T398I[7]
23 p.I36M[8]
24 p.I46M[9]

Nonsense mutations

8 p.Y232X[7]
11 p.R240X[3]
22 p.R125X

Missense/Insertion

3 p.A98G_V99insT[7]

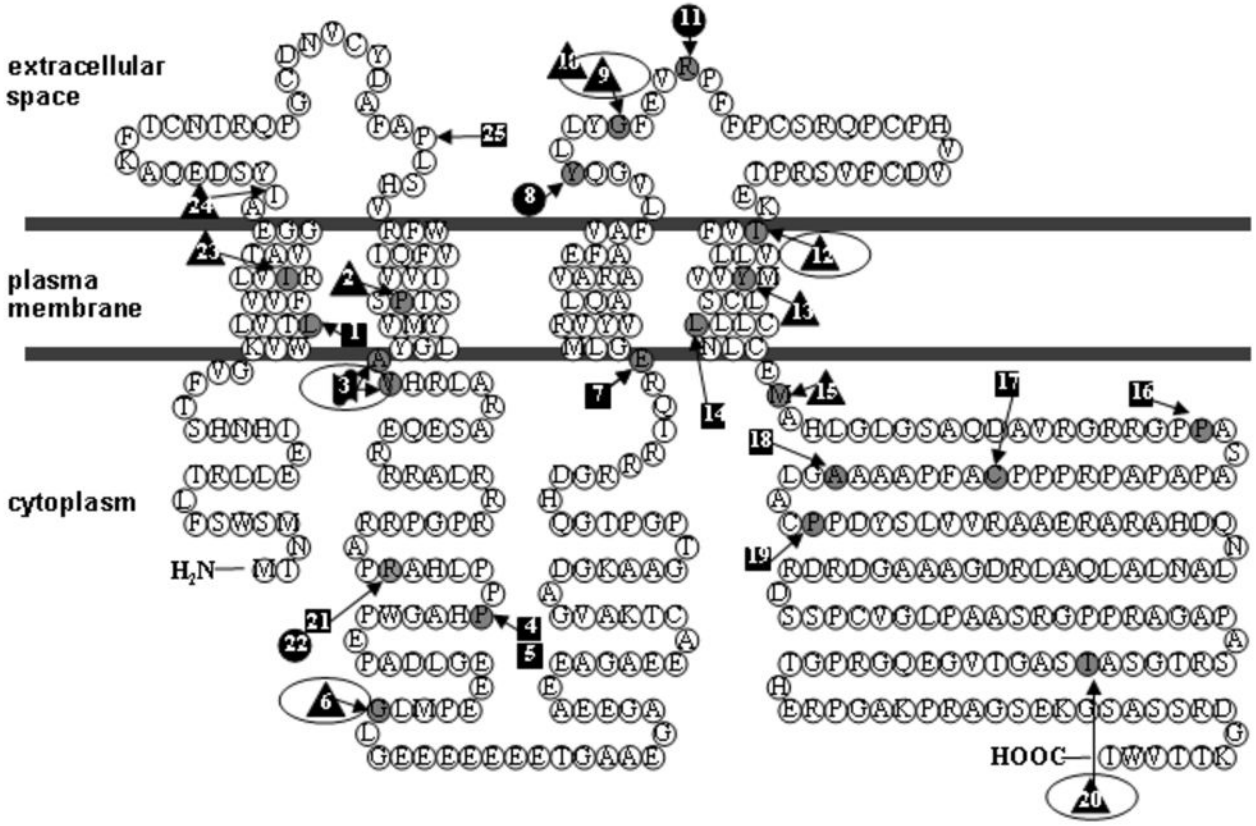

HeLa
Cx47WT
T398I
G149S
A98G_V99insT
G236R
T265A
49
38
α Cx47
α GAPDH

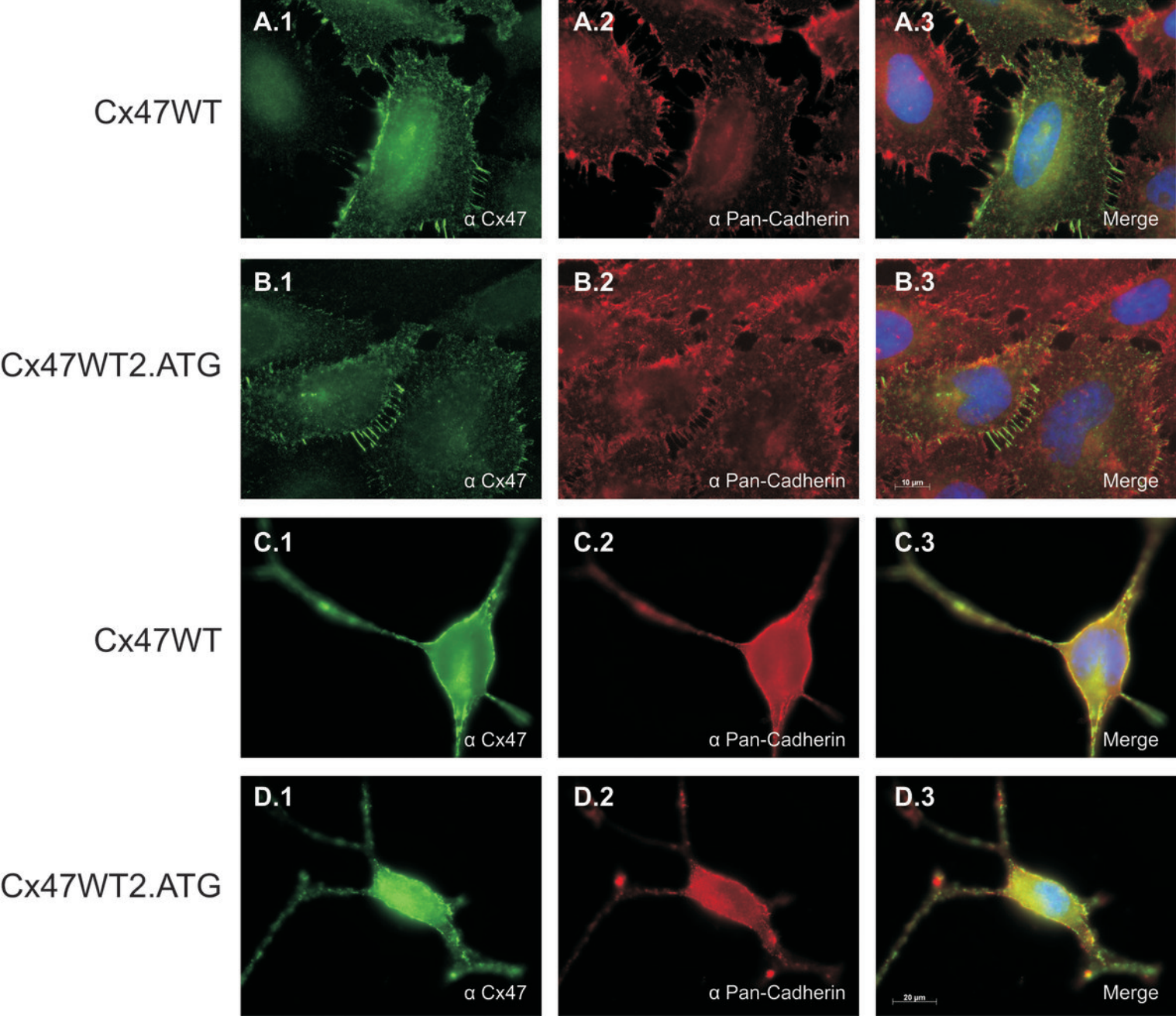
Cx47WT
A.1
α Cx47
A.2
α Pan-Cadherin
A.3
Merge
Cx47WT2.ATG
B.1
α Cx47
B.2
α Pan-Cadherin
B.3
10 µm
Merge
Cx47WT
C.1
α Cx47
C.2
α Pan-Cadherin
C.3
Merge
Cx47WT2.ATG
D.1
α Cx47
D.2
α Pan-Cadherin
D.3
20 µm
Merge

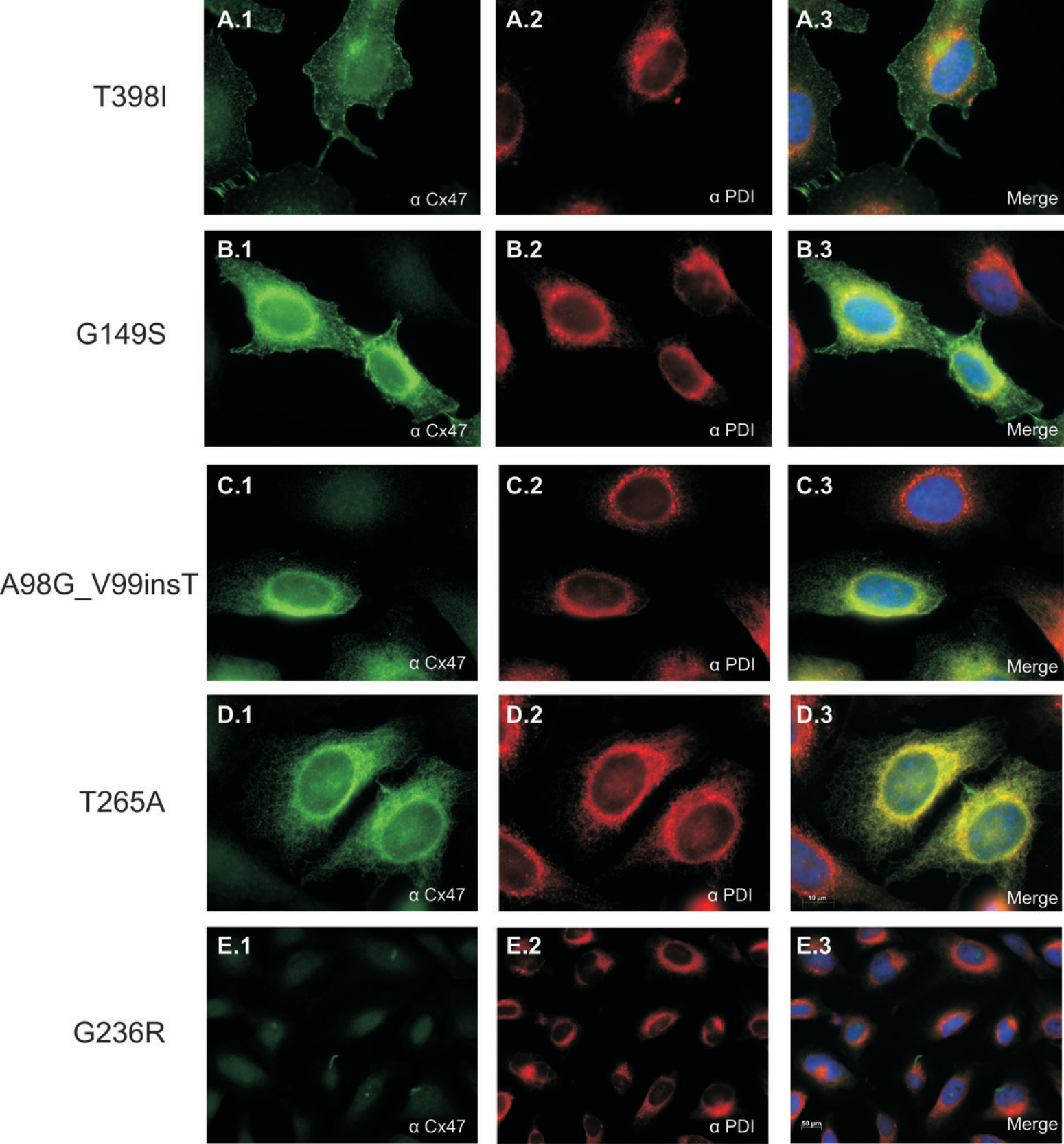
T398I
A.1
α Cx47
A.2
α PDI
A.3
Merge
G149S
B.1
α Cx47
B.2
α PDI
B.3
Merge
A98G_V99insT
C.1
α Cx47
C.2
α PDI
C.3
Merge
T265A
D.1
α Cx47
D.2
α PDI
10 µm
D.3
Merge
G236R
E.1
α Cx47
E.2
α PDI
50 µm
E.3
Merge

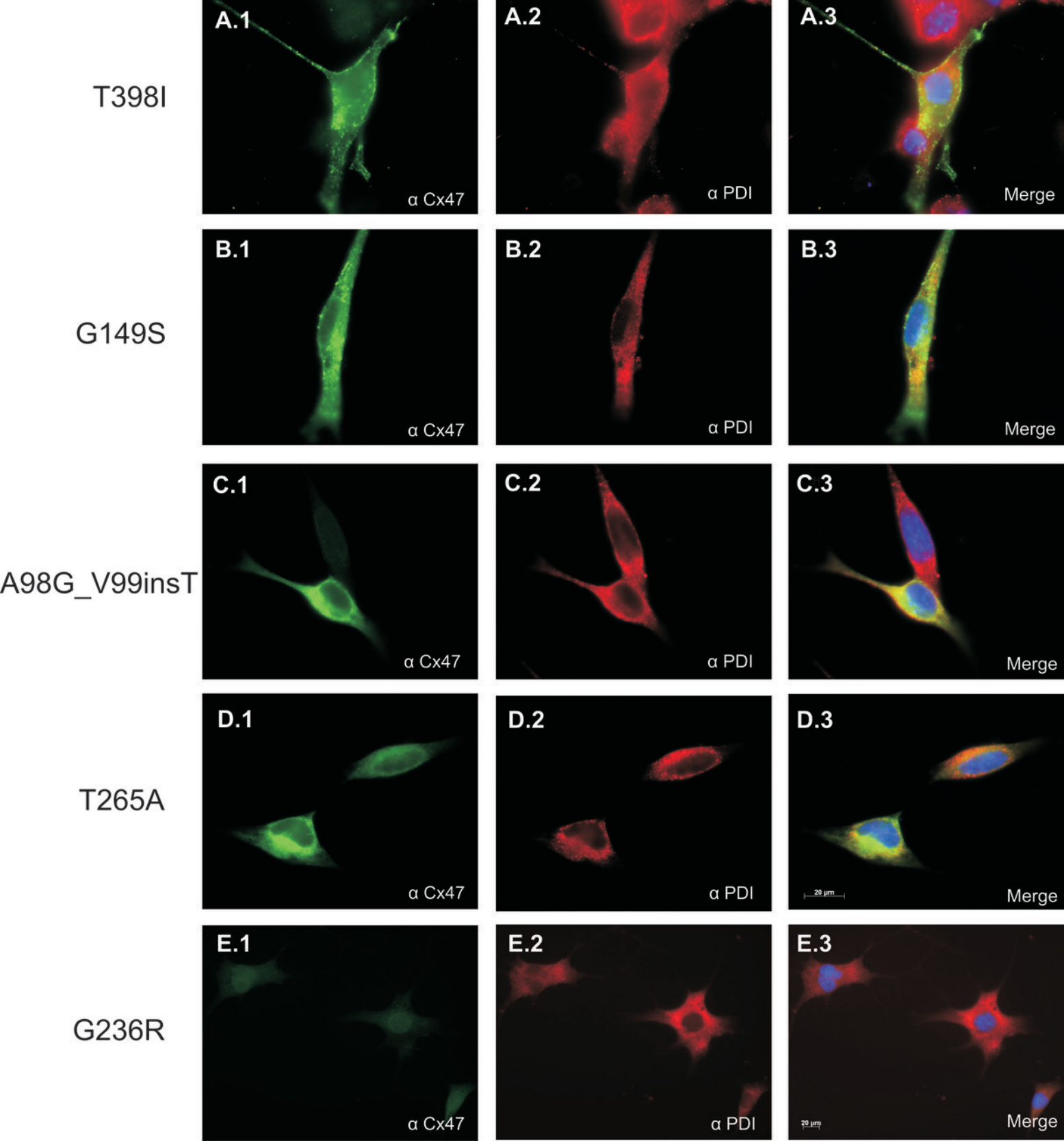
T398I
A.1
α Cx47
A.2
α PDI
A.3
Merge
G149S
B.1
α Cx47
B.2
α PDI
B.3
Merge
A98G_V99insT
C.1
α Cx47
C.2
α PDI
C.3
Merge
T265A
D.1
α Cx47
D.2
α PDI
D.3
20 µm
Merge
G236R
E.1
α Cx47
E.2
α PDI
E.3
20 µm
Merge

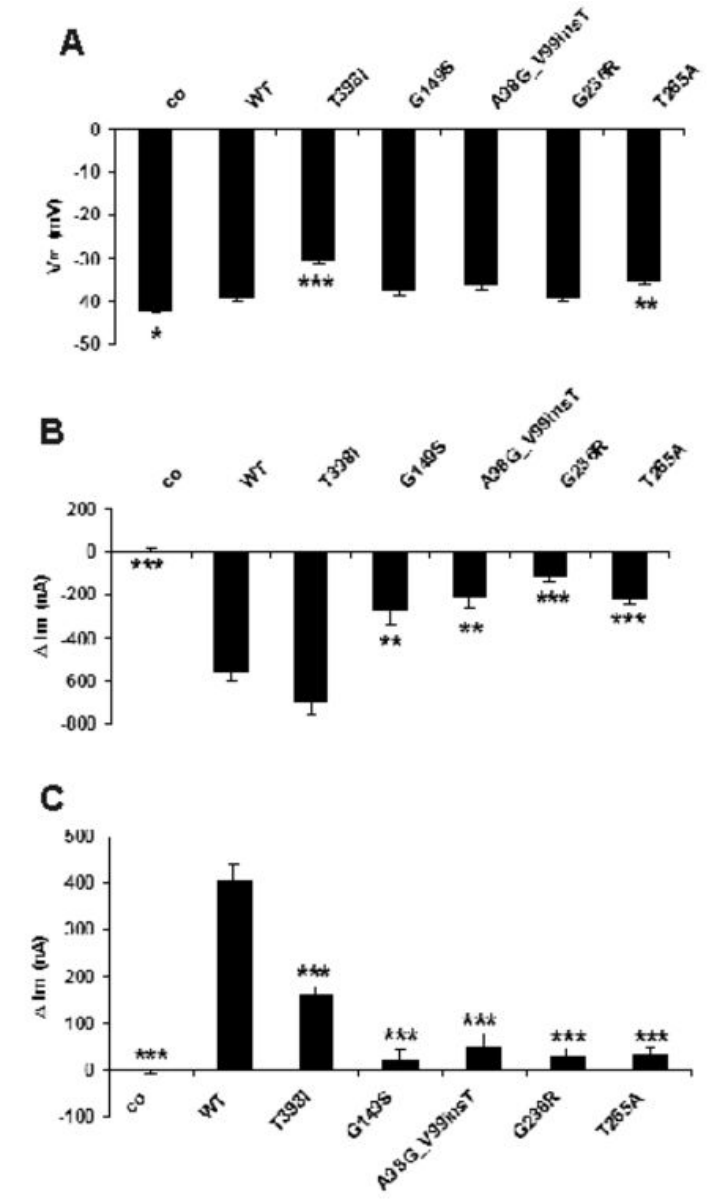
A
co
WT
T393I
G149S
A98G_V99insT
G236R
T265A
0
-10
-20
-30
-40
-50
Vm (mV)
*
***
**
B
co
WT
T393I
G149S
A98G_V99insT
G236R
T265A
200
0
-200
-400
-600
-800
Δ Im (nA)
***
**
**
***
***
C
500
400
300
200
100
0
-100
Δ Im (nA)
***
***
***
***
***
co
WT
T393I
G149S
A98G_V99insT
G236R
T265A

Table 1 Clinical data of patients and functional consequences of Cx47 mutations.

Patient/ Sex	Age at disease onset, mo	Age at last examination	Score of best motor function[1] (age at walking, y)	Speech (age>1 y)	Education (age>5 y)	Course	Age at onset of motor degradation, y	Age at onset of speech deterioration, y	Mutation at nucleotide level	Mutation at protein level	mutant alleles	localization of Cx47	functional defect of Cx47
mt3548/M	9	7	1	+ (D)	Special school	S	-	-	c.1193C>T	p.T398I	het	PM	dysfunction
G218/M	12	6	4 (2)	+ (D)	Regular school	SD	5	-	c.1193C>T	p.T398I	het	PM	dysfunction
G344/M	3	1	2			SI	-	-	c.445G>A	p.G149S	het	ER, PM	loss-of-function
mt3550/M	9	5	2	+	Special school	S	-	-	c.292_293 insGTA	p.A98G_V99 insT	het	ER	loss-of-function
G330/F	1	17	4 (3,5)	+ (D)	Regular school	SD	8 (wcb 10)	11	c.793A>G	p.T265A	hom	ER	loss-of-function
G193/M	12	14	2	+ (D; BD)	Special school	SD	4	12	c.706G>C	p.G236R	hom	ND	loss-of-function

Mutations and clinical data previously described and published by our group.[7] Mutation nomenclature is based on GJA12/GJC2 cDNA sequence (RefSeq NM_020435.2), +1 corresponds to the A of the first ATG.

[1] Disease forms according to a development score (best motor function acquired): 0 = no motor achievement; 1 = head control; 2 = sitting without aid; 3 = walking with aid; 4 = walking independently.

BD = buccofacial dyspraxia; D = dysarthria; S = stable; SD = slow degradation; SI = slow improvement; wcb = wheelchair bound; het = heterozygous; hom = homozygous; ER = endoplasmatic reticulum; PM = plasma membrane; ND = not detectable.